

KINETICS OF THE GAS PHASE REACTION
BETWEEN
NITRIC OXIDE, NITROGEN DIOXIDE AND WATER VAPOR

Thesis by
Lowell G. Wayne

In Partial Fulfillment of the Requirements
for the Degree of
Doctor of Philosophy

California Institute of Technology
Pasadena, California

1948

ACKNOWLEDGEMENTS

The author is grateful to Dr. Don M. Yost for his inspiration and guidance, and to Dr. Oliver Wulf and Dr. Norman Davidson for their generous suggestions and discussions concerning the research herein described.

A grant by the Allied Chemical and Dye Company made possible the completion of this work.

ABSTRACT

Using the absorption of light by nitrogen dioxide as a measure of its concentration, the rate of the reaction $\text{NO}_2 + \text{NO} + \text{H}_2\text{O}(\text{g}) \rightleftharpoons 2\text{HNO}_2(\text{g})$ has been measured over a five-fold range of water vapor and nitrogen dioxide concentrations, with nitric oxide greatly in excess. Changes in light intensity were detected by means of an electron-multiplier phototube and recorded by photographing the screen of a cathode-ray oscilloscope. Half-times as short as 0.014 sec. were observed. The reaction rate was found to depend more strongly upon the concentration of water vapor than upon that of nitrogen dioxide and to be kinetically consistent with a mechanism involving termolecular collisions.

As incidental results of the study, the equilibrium constant of the above reaction has been calculated and its order of magnitude experimentally confirmed, and a lower limit has been fixed for the rate of dissociation of nitrogen sesquioxide.

TABLE OF CONTENTS

I.	INTRODUCTION	1
II.	EXPERIMENTAL	2
	A. General	2
	B. The flow system	2
	C. The reaction system	5
	D. The optical system.	6
	E. The detecting and recording system	7
	F. The procedure	7
	G. Calibration of the detecting system	8
	H. The photographs	10
	J. Further remarks concerning the apparatus.	11
III.	THE EQUILIBRIUM CONSTANT	13
	A. Thermodynamic calculation	13
	B. Confirmatory evidence	15
IV.	ORDER OF THE REACTION.	19
	A. Characteristics of the rate curve	19
	B. Derivation of the order tests	22
	C. Discussion of the approximations.	25
	D. The results	30
V.	CONCLUSIONS.	36
	A. The rate constant	36
	B. Comparison with kinetic theory	37
	REFERENCES.	41

I. INTRODUCTION

Following the successful application by Johnston (1) of the combination of multiplier phototube, cathode-ray oscilloscope and camera to the study of the kinetics of the very rapid reaction between nitrogen dioxide and ozone, it appeared desirable to study by this technique other reactions whose rates are so great as to be unmeasurable by the common methods. The reaction between nitric oxide, nitrogen dioxide and water vapor, which is also of interest because of its possible importance in connection with theories of rainfall, appeared to fall in this category. Dr. Oliver Wulf, who had studied the equilibrium in this reaction spectroscopically (2), testified that equilibrium was attained practically instantaneously.

Instances in the literature of the quantitative study of kinetics of homogeneous reactions involving water vapor as a primary reactant are rather rare, and most of these concern pyrolysis of hydrocarbons or other high temperature studies in which the effect of chain reactions is predominant. The reaction between water vapor and sulfur trioxide in the gas phase was studied (3) at room temperature by the Polanyi streaming method; in this case, of course, the product, sulfuric acid, appeared as a mist. The authors estimated that about one collision out of every hundred between molecules of the reacting species was effective, so that the reaction was extremely fast. The system proposed here is comparable to the water-sulfur trioxide system at least in the respect that it, too, involves

an acid anhydride, namely, nitrous anhydride or nitrogen sesquioxide, which is always present in equilibrium with nitric oxide and nitrogen dioxide in their mixtures.

II. EXPERIMENTAL

A. General.

In principle and in many particulars the procedure was the same as that employed by Johnston (loc.cit.). Essentially the apparatus comprises four parts: a flow-system in which gas streams containing the reacting substances could be metered and mixed, a device consisting of a reaction cell and stopgate by means of which a non-equilibrium mixture could be trapped, an optical system producing a beam of light which passed through a portion of the reaction cell, and a detecting and recording system comprising the multiplier phototube with its power source, the oscilloscope and the camera.

B. The flow system.

Figure 1 shows schematically the arrangement of the flow system. Nitric oxide, prepared as described below, entered the system at A, filled the two-liter bulb B (which served to cushion the effect of suddenly closing the system) and was divided into two streams. One of these passed through stopcock C, flowmeter D and water saturator E, the other through stopcock F and flowmeter G to H, where a much slower stream of oxygen was introduced. The stopcocks J and K permitted these sections of the flow system to be cut off from

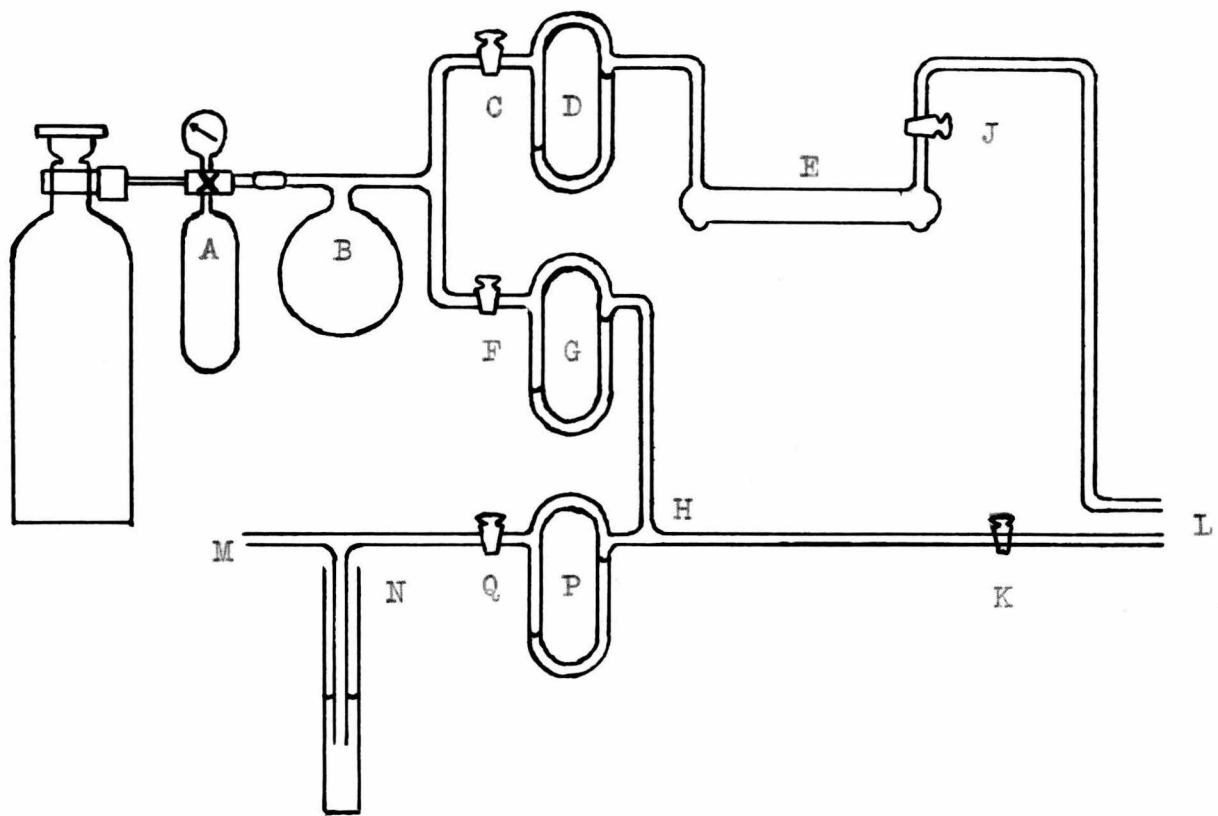


Figure 1. Diagram of the flow system

A, nitric oxide collecting system

B, two liter bulb

D, G, P, capillary flowmeters

E, water saturator

L, to mixing chamber

M, oxygen inlet

N, bubbler

the mixing chamber L and from each other. Oxygen from a commercial oxygen cylinder was introduced at M; its pressure was adjusted by means of the bubbler N and its flow rate measured by flowmeter P. Stopcock Q served to shut off the oxygen stream.

Dibutyl phthalate was used as the manometer fluid in capillary flowmeters D, G and P, which were of the usual construction except for a stopcock which had to be inserted in the left arm of manometer P to prevent the accumulation of dissolved N_2O_3 with resultant imbalance in the absence of flow. The capillaries were calibrated at several points throughout their ranges of utility by timing the displacement of a known volume of water. (Suitable corrections were made to allow for the vapor pressure of water; solubilities of nitric oxide and of oxygen in water were neglected.)

Water saturator E consisted of a 120 cm. length of 12 mm. tubing bent to sit flat and filled with glass beads and sufficient water to occupy half the remaining volume. It was kept immersed in water at room temperature. A gravimetric water vapor determination showed it to be more than 99% efficient at the flow rates used.

Mixing chamber L (Fig. 2a) was of the same construction as that used by Johnston (loc. cit.), with the two streams being introduced tangentially and the mixture flowing out centrally. The volume of the mixing space was ca. 0.05 cm^3 , as indicated by the weight of acetone it held.

Bubbler N consisted simply of a tube immersed to an ad-

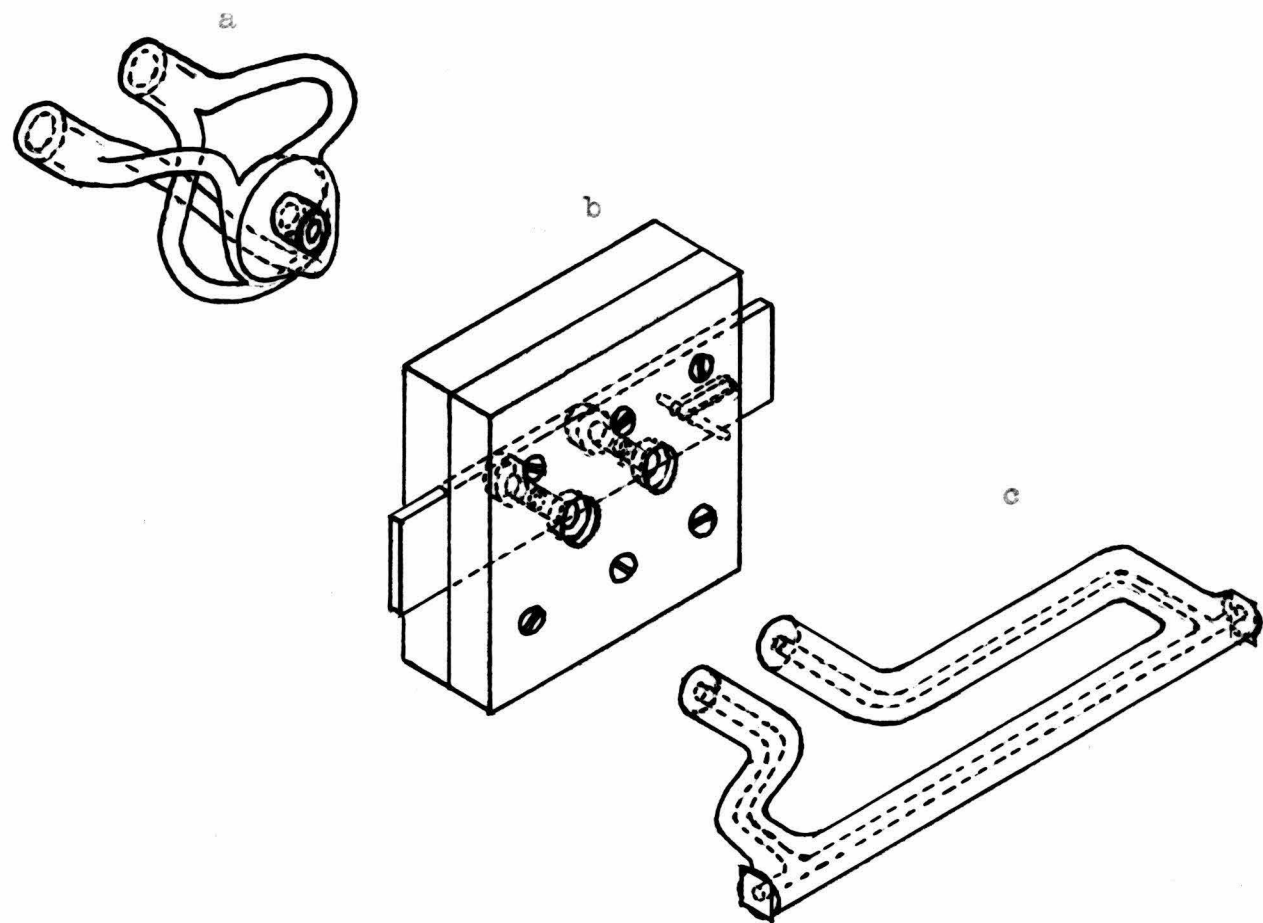


Figure 2; a, the mixing chamber
b, the stopgate
c, the reaction chamber

justable depth in a column of water.

The concentration of water vapor in the reaction mixture could be adjusted by diverting more or less of the total nitric oxide flow through stopcock C; the concentrations obtainable in this way ranged from about 0.5 to about 2.4 mole percent. The total nitric oxide flow rate was fixed by setting the valve on the supply cylinder.

The temperature of the flowing mixture was measured by means of a thermocouple of #30 B & S constantan and 36 gauge copper placed axially in the stream issuing from the reaction cell. No attempt was made to control the temperature, which therefore varied slowly, usually between 23 and 25°*C*.

Tygon tubing was used for all connections. As it was found that this tubing was slowly attacked by nitrogen dioxide, connections were arranged so as to expose a minimum of the tygon surface to the stream containing this component.

For the experiments concerning possible time lag in the NO_2 - N_2O_3 equilibrium, the water saturator was removed from the system and nitrogen from a commercial "dry nitrogen" cylinder was introduced into the mixing chamber.

Nitric oxide was generated by the method given by Johnston and Giauque (4), in which 50% sulfuric acid is dropped into a solution approximately 4N in Sodium nitrite and 1N in potassium iodide. The gas evolved was passed consecutively through three washing bottles, the first contained concentrated sodium hydroxide solution, the others saturated potassium iodide--then through a drying tower containing phosphorus pentoxide

and a cold trap immersed in a bath of dry ice and isopropyl alcohol and was finally condensed in a glass bulb at liquid-air temperature. It was then redistilled (the last five percent or so of each batch being discarded), into a steel and brass collecting system (A, Fig. 1) attached to the supply cylinder, which was of the type used for oxygen. (At room temperature one mole of gas produced a pressure of about 100 pounds per square inch in this system.) The only likely impurity in the gas thus produced was nitrous oxide. No nitrogen dioxide could be detected.

C. The reaction system.

Pyrex 1mm capillary tubing served for the reaction chamber, constructed in the form shown in figure 2c. The total length of tubing was about 15 cm., the length of the light path about 6 cm. and the length preceding the light path about 3 cm. The total volume of the reaction chamber was thus ca. 0.12 cm^3 , the volume between the inlet and the center of the light path 0.05 cm^3 .

Pieces of microscope cover slips served as optical windows for the straight portion of tubing which provided the light path. These were stuck on with a thin layer of de Khotinsky cement which also cut out any light which might otherwise have been transmitted lengthwise through the glass. The entrance and exit ends of the chamber were ground to fit closely into countersunk holes in the stopgate block.

The stopgate, (fig. 3b) constructed of stainless steel, comprised a thin slide machined to fit between two blocks in

such a way that two channels through the system could be opened or closed simultaneously by movement of the slide. The mixing chamber and the reaction cell were affixed in countersunk holes in the blocks by means of "Insalute" cement and bolstered with liberal quantities of paraffin. The whole was mounted, with the light path approximately horizontal, on a 20-pound lead block equipped with thumb screws to facilitate adjustment. In operation the stopgate was closed by a "snapper" consisting of a 20 gram bronze block on one end of a 10 cm. strip of spring brass, the other end of the strip being fixed on the side of the lead block.

D. The optical system.

Light from a 500 watt G.E. Mazda projection lamp (rated for 120 v but operated at 68 v) was passed through yellow and blue filters to isolate a relatively narrow wavelength region (maximum intensity at 4500 \AA , half-width about 400 \AA°) which is particularly strongly absorbed by NO_2 . A pair of condensing lenses focussed the filtered light on a pinhole (in 30 gauge copper sheet) from which issued a divergent beam. A small lens intercepted the light from the center of this beam (avoiding the diffraction ring) and focussed it near the proximal end of the reaction cell.

The optical system, except for the small lens, was mounted on an adjustable base so that position and direction of the emergent beam relative to the reaction chamber could be changed. Suitable settings to minimize the effects of the mechanical disturbance of closing the stopgate and to provide

a convenient amount and intensity of light for the measurements were obtained manually by trial and error.

E. The detecting and recording systems.

An RCA 1P21 electron multiplier phototube served to measure the intensity of light emerging from the reaction chamber. Voltage for the operation of the tube was provided by a set of sixteen $67\frac{1}{2}$ v. Minimax batteries. A 900,000 ohm voltage divider furnished 90 volt steps between successive dynodes and between dynode #9 and the anode. For the elimination of high frequency noise, an R-C filter was inserted in connection with the output of the tube. (This circuit is diagrammed in Fig. 3.) The signal from the tube was conveyed to a cathode-ray oscilloscope (Du Mont Type 247) having a 5-inch screen giving a "high actinic" trace. A light-chopping disc with 10 openings, rotated by a synchronous motor at 1800 r.p.m., was so placed as to interrupt the light beam between the pin-hole and the small collecting lens, thus providing in the signal produced by the phototube a 300 cycle a.c. component, with amplitude proportional to the intensity of transmitted light.

The screen was photographed with the aid of a Mercury II camera having an f-2.7 lens which was set forward about 1/16 inch so as to focus satisfactorily when used at a distance of about 12 inches from the screen.

F. The procedure.

To make and record a single run, after the desired steady state had been attained in the flow system and the pattern adjusted to a satisfactory position on the screen, the

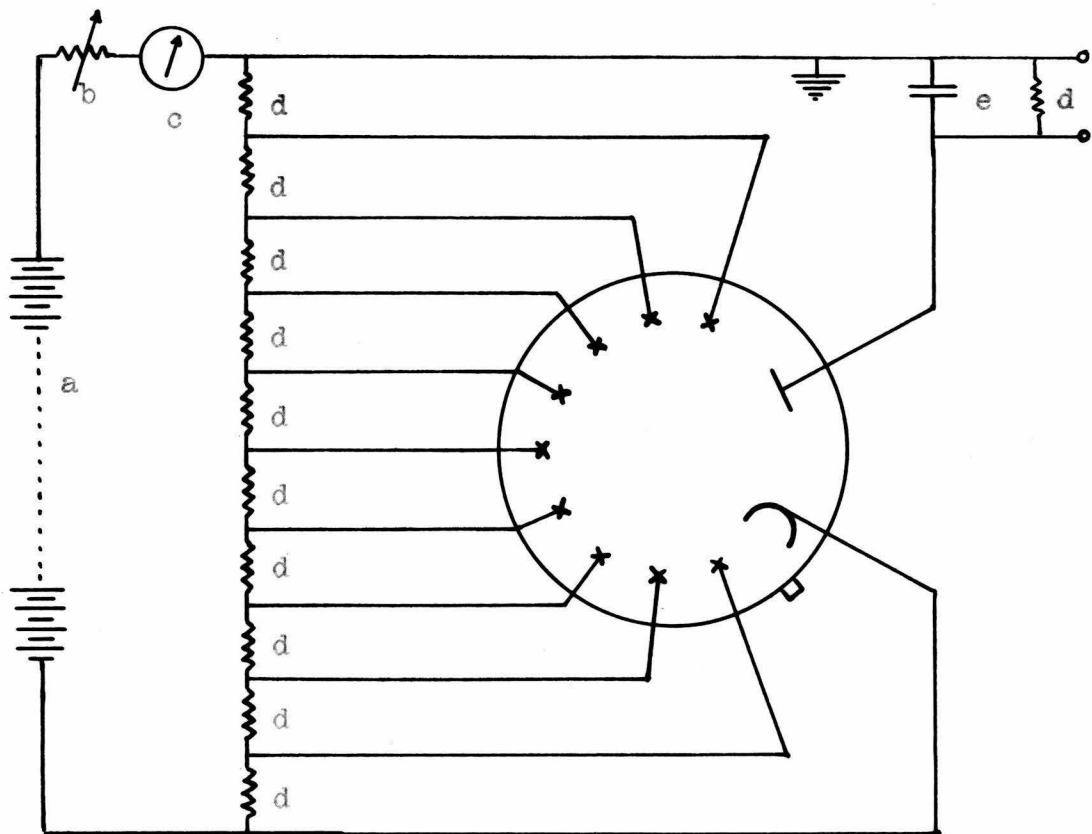


Figure 3. Circuit for the operation of the multiplier phototube

- a. 1200 volts d. c.
- b. 200,000 ohms
- c. zero to one milliampere
- d. 90,000 ohms
- e. 0.01 microfarad

operator in rapid sequence opened the camera shutter, sprang the snapper to close the stopgate, then closed the shutter. It was found that these operations could be completed in one half second or less and the necessity of using the single-sweep feature of the oscilloscope was avoided. This procedure had the additional advantage that each photograph so taken showed the position of the pattern before the gas flow was interrupted, thus automatically providing a blank for each run. However, in the experiments on dilution of N_2O_3 the single sweep circuit was used, triggered by the movement of the snapper; blanks were made separately.

After each run the stopgate was quickly opened to avoid excessive pressure in the flow system. New flow settings were then made, if desired, and in the interim while a new steady state was being established, flowmeter and temperature readings and new oscilloscope settings were made. The time necessary for attainment of the steady state was usually one or two minutes, depending on the total rate of flow of nitric oxide, which was ordinarily between 5 and 10 cubic centimeters per second.

G. Calibration of the detecting system.

Since it was desirable to use the detecting system under conditions such that its response to change of light intensity would be approximately linear, the arrangement devised was tested by inserting various calibrated screens in the light path and measuring the amplitude of the resulting pattern on the oscilloscope screen. When the voltage applied

across the projector lamp was 70 v. or less, response was satisfactorily linear. Throughout the experiments this condition was met.

In order to magnify the observable effect produced by reaction occurring in the chamber, it proved useful to set the oscilloscope controls so that only the lower edge of the pattern was observed on the screen. A further calibration was necessary to relate the data thus obtained to the intensity of the light transmitted through the reaction chamber. It was found that when the vertical positioner was set at its extreme clockwise position, the position of the pattern edge could be correlated (within about 5%) with the applied signal by assuming the center of the pattern to be 5.0 inches above the center of the screen and its amplitude proportional not only to the intensity of light incident on the phototube but also to the setting of the Y-gain knob, so long as this varied within the rough limits 15 to 60. These assumptions were used in estimating the equilibrium constant from the photographs but were unnecessary in finding the half-time and rate corresponding to any particular run. In this connection it is to be noted that the full amplitude increase produced by a sudden change in intensity was observable at the lower edge of the pattern, since the increase in amplitude of the a.c. component of the signal was matched by a proportional sudden increase of the d.c. component. The position of the upper border of the pattern, corresponding to the dark period of the intensity cycle, was only affected more slowly as the center drifted back to its equilibrium position.

To avoid distortion due to the curvature of the screen, the pattern was usually adjusted so that its lower edge prior to reaction was slightly above the center of the screen. To insure the measurability of the position of this edge on the photograph, a strip of cellulose tape marked in India ink provided a frame of reference directly on the screen. Tests showed that the distortion due to curvature was not important in comparison with the random variability of the amplitude of the pattern.

Johnston (loc. cit.) found that with light filtered as described above, nitrogen dioxide obeyed Beer's Law. This finding was confirmed with the system used in the present work. The readings obtained with given total concentrations of available nitrogen dioxide^{were} not accurately reproducible because in the presence of nitric oxide at atmospheric pressure approximately one third of the total is sesquioxide, the exact ratio varying slightly with the temperature. Nevertheless the calibration of the system against total available nitrogen dioxide was useful in permitting the confirmation of the calculated equilibrium constant for the reaction under study.

H. The photographs.

The photographic negative, on 35 mm. Plus-x film, produced an image of the oscilloscope screen having a diameter of about 10 mm. The pattern produced on the screen by each sweep of the electron beam across the cathode ray tube somewhat resembled an inverted picket fence (as seen in figures 4c and 4d, for which the single sweep apparatus was used); in general,

three or four of these appeared in superposition, as in figures 4a and 4b.

For measurement, the image was projected in a microfilm reader onto a sheet of squared paper and the positions of successive peaks recorded. The magnification factor between screen and tracing was found to be 2.4. The interval between successive points corresponded, of course, to a time lapse of 1/300 of a second.

J. Remarks concerning the apparatus.

It was apparent that the apparatus used in this study is susceptible of considerable improvement, looking toward its use in securing more accurate data and in studying even faster reactions. The usefulness of the data obtained in this investigation was limited because of both mechanical instability of the optical system and random variability in the response of the detecting system.

The mechanical instability of the optical arrangements was found to be due principally to the thumb screws with which the lead block supporting the reaction cell had been equipped in order to make the direction of the cell readily adjustable. These allowed some vibration of the block (and therefore of the cell) relative to the light beam, and although this was painstakingly minimized by trial and error adjustment before making a set of runs, the effect was clearly visible in the photographs as a disturbance of frequency about 30 to 40 per second. It is believed that the system used for snapping the stopgate shut (as described in section C above) is not directly responsible

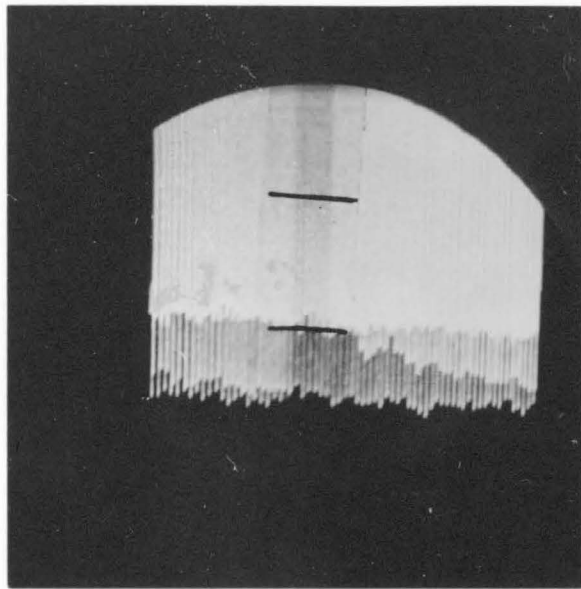


Figure 4a. Run IV-59
 N_2O_3 0.0078 atm.,
 H_2O 0.0151 atm.;
half time 0.083 sec.

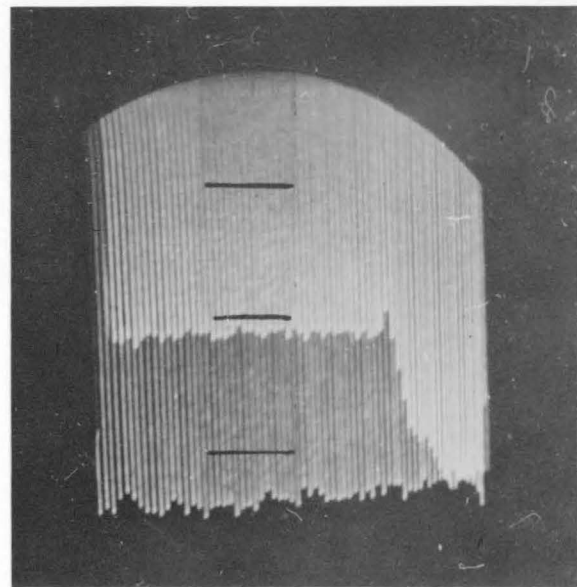


Figure 4b. Run IV-52
 N_2O_3 0.0148 atm.,
 H_2O 0.0230 atm.;
half time 0.014 sec.

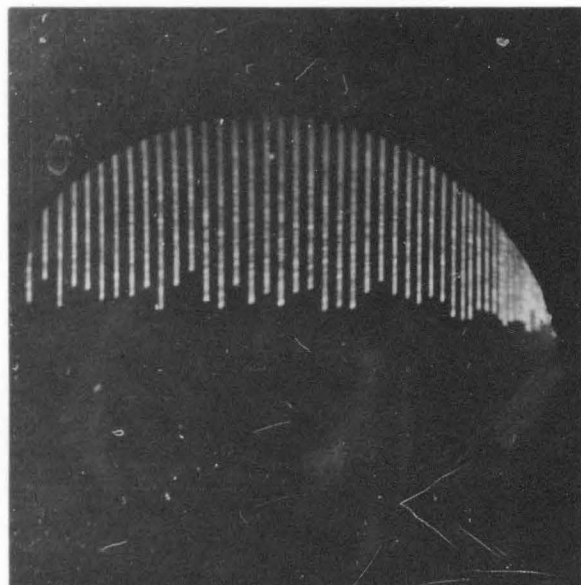


Figure 4c. Blank for N_2O_3
dilution test

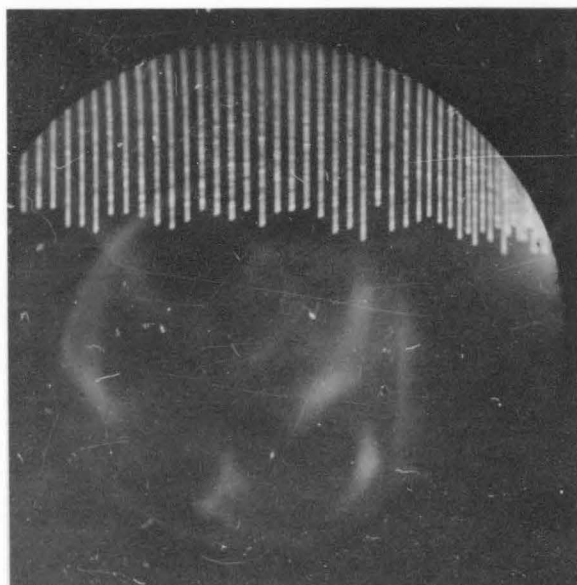


Figure 4d. N_2O_3 dilution test,
 N_2/NO , 4.5

for this pronounced effect. The primary problem, therefore, is to arrange the reaction cell to be adjustable with respect to its mounting but vibrationless when fixed thereon.

The variability in response of the detecting system is of two sorts: (1) a high frequency variability which causes the raggedness of the pattern edge, as seen in figures 4c and 4d, and (2) unpredictable but substantial changes in the magnitude of the response to a given light intensity. The first sort can apparently be traced, at least in part, to the influence of "noise" produced by thermionic emission of electrons from the sensitive surface of the multiplier phototube and by statistical variations in the random process of secondary emission⁽⁵⁾. This effect can reportedly be much reduced by operating the phototube at a low temperature.⁽⁶⁾ The second sort includes changes due to fatiguing of the sensitive surface, the voltage source for the dynodes, and the response of the oscilloscope to imposed signals, as well as discontinuous changes which are probably due in the main to the very slight variations in the D.C. line voltage to the light source but are certainly due in some cases to erratic behaviour of the oscilloscope. In the current investigation the method of analysis of the data obviated to a large extent the requirement of long-interval stability of the system, but such stability is desirable in any event.

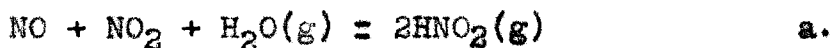
In addition, it is clearly desirable to obtain runs at temperatures different from that of the room, for which purpose as much of the flow system as possible should be thermo-

stated. This would probably require construction of an air thermostat to enclose the reaction cell, stopgate and mixing chamber and of an efficient heat exchanger in the flow system to bring the reacting gases to the desired temperature before they enter the mixing chamber.

III. THE EQUILIBRIUM CONSTANT

A. Thermodynamic calculation

Because the reaction



does not proceed to completion but reaches equilibrium with appreciable amounts of the reactants remaining in the system, a knowledge of its equilibrium constant is essential in interpreting its kinetics. Abel and Neusser (?), in measuring the vapor pressure of nitrous acid above its aqueous solutions, also encountered this problem; on the basis of equilibrium data then available they calculated the quantity

$$cK_i = \frac{P_{\text{NO}_2}}{(\text{HNO}_2)^2} \approx 1.7 \times 10^{-2} \quad \text{lit. atm. / mole}^2$$

at 25°C, the gas phase being saturated with water vapor. Introducing the pressure of water vapor and the factor

$$c k = \frac{P_{\text{HNO}_2}}{(\text{HNO}_2)} = 0.0352 \quad \text{lit. atm. / mole}$$

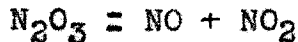
determined by these authors one readily calculates for the reaction



the dimensionless equilibrium constant

$$K_b = (c_k)^2 / c K_c \cdot P_{H_2O} = 2.4$$

combining this with the value $K_c = 2.1$ atm. found by Verhoek and Daniels (8) for the dissociation



c.

gives $K_a = K_b / K_c = 1.2 \text{ atm}^{-1}$

In calculating the value given above for $c K_c$ Abel and Neusser found it necessary to employ the estimated figure

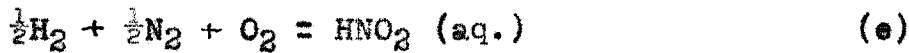
$$c K_c = \frac{(H^+)(NO_3^-) P_{NO_2}^2}{(HNO_2)^3} = 100 \text{ l. atm}^2/\text{mole}$$

obtained as an incidental result of their experiments. They pointed out that only the order of magnitude of this figure was established, since the experiments were not designed to provide an accurate determination; indeed, the individual results range from about 50 to more than 300. It is perhaps indicative of the authors' uncertainty on this score that, although their calculations showed that in a typical run approximately 10% of the trivalent nitrogen in the vapor phase would be N_2O_3 , they made no attempt to correct for this error in either the individual experiments or the final average value of c_k , which is therefore presumably too high by 10 to 20 per cent.

Thermodynamic data now available permit a more reliable calculation. The result still depends upon the vapor pressure data of Abel and Neusser and is therefore subject to the same

10 to 20 per cent uncertainty, but the much more refined treatment of the thermodynamic properties of nitric acid given by Forsythe and Giauque (9) removes the order-of-magnitude uncertainty inherent in the above estimate.

Consider the reactions



Combining these in the proportions 2(d) + 2(e) - (f) - (g) - (h) yields the net reaction (a). Extrapolation of the results of Abel and Neusser to ionic strength zero gives $K_d = 0.0305$, from which ΔF_d° is calculated to be 2,080 cal./mole. The standard free energy changes for (f) and (g), taken from Forsythe and Giauque, are $\Delta F_f^{\circ} = 12,275$, $\Delta F_g^{\circ} = 20,650$; from Latimer (10), $\Delta F_g^{\circ} = -13,020$, and from Lewis and Randall (11), $\Delta F_h^{\circ} = -54,507$. Thus for the reaction in question, $\Delta F_a^{\circ} = 2 \times 2080 - 2 \times 13020 - 12275 + 20650 + 54507 = -300$ cal./mole, and $K_a = \frac{P_{\text{HNO}_2}}{P_{\text{NO}_2} P_{\text{NO}_1} P_{\text{H}_2\text{O}}} = 1.65 \text{ atm.}^{-1}$ in reasonable agreement with the value calculated from the data of Abel and Neusser. Multiplying by K_c gives $K_b = K_a K_c = 3.5$.

B. Experimental confirmation.

Because of the technique involved, the data reported in this investigation were not well suited to the calculation

of equilibrium constants. A particular difficulty was that the intensity of transmitted light had to be estimated from the amplitude of the pattern, of which only one edge was visible on the screen, while the position of its center was subject to a slow drift. Nevertheless, such estimates as could be carried out confirmed for K_e and K_c the order of magnitude found in the above calculations. A single example will show the method employed.

In view of the fact that all runs were carried out in the presence of a large excess of nitric oxide, its pressure could be considered constant and the ratio of N_2O_3 to NO_2 in these systems also constant. Neglecting the small pressure of N_2O_4 , therefore, the actual concentration of NO_2 in the reaction cell was always proportional to the total pressure of $NO_2 + N_2O_3$, which is henceforth, for convenience, called "available" N_2O_3 in recognition of the essentially instantaneous establishment of equilibrium between these gases. Denoting this quantity by $P_{[N_2O_3]}$, one obtains

$$P_{[N_2O_3]} = P_{NO_2} + P_{N_2O_3} = P_{NO_2} \left(1 + \frac{P_{NO_2}}{K_c}\right)$$

It is also convenient to define the "equilibrium constant" involving this quantity, taking $P_{NO} = 1$, as

$$K = \frac{P_{NO_2}^2}{P_{[N_2O_3]} P_{H_2O}} = K_e P_{NO} P_{NO_2} / P_{[N_2O_3]} = 1.65 / 1.5 = 1.1.$$

In what follows, the term "equilibrium constant" will refer to K thus defined, unless otherwise specified.

Run IV-52 provides particularly suitable conditions for

estimating the equilibrium constant for several reasons. First, the half-time found was very short (about 0.014 second), so that equilibrium could be established before the drift of the pattern became appreciable. Second, the measured effect was large, so that the uncertainty introduced in calculating P_{HNO_3} by difference was relatively small. Finally, this run was immediately followed by a "dry run" in which the initial $P_{H_2O_3}$ was practically the same but P_{H_2O} was zero, thus furnishing a reasonably secure reference point for the calibration of the scope response.

Between $P_{H_2O_3}$ and the oscilloscope readings, there existed the general relation, previously established by calibration (cf. Sec. II-G):

$$P_{H_2O_3} = \frac{1}{16} \log \frac{sG}{\alpha} \quad (1)$$

where G denotes the Y-gain setting, α the amplitude of the pattern, and s an adjustable factor to account for changes in the response of the phototube or oscilloscope, or in the intensity of the light source. The dry run IV-53, with $P_{H_2O_3} = 0.0151$ and $G = 20$, gave $\alpha = 20.4$, from which is calculated to be 1.78. (α here is given in terms of the theoretical width of the entire pattern on the tracing on the assumption that magnification is linear. In this case the edge of the pattern was found to be 3.2 inches below the reference point of the tracing; the center of the pattern was calculated to be 7.0 inches above this reference point, so the amplitude was $2 \times (3.2 + 7.0)$ or 20.4 inches).

For run IV-52 the initial concentrations were

$P_{[N_2O_3]_i} = 0.0148$ and $P_{H_2O_i} = 0.0230$; the total rate of flow was $7.1 \text{ cm}^3/\text{sec.}$, so that the gas in the light path had traveled an average of 0.014 seconds after mixing (the volume of the mixing chamber plus half that of the reaction chamber being estimated as 0.10 cm^3 ; see Section II-C). From the tracing, the amplitude corresponding to the steady state is found to be 23.0 inches and the maximum displacement of the pattern edge 3.0 inches (again with Y-gain 20). Hence α is assigned the value 26.0 and from (1), the available NO_2 at equilibrium has the pressure

$$P_{[N_2O_3]_\infty} = \frac{1}{16} \log \frac{1.78 \times 20}{26.0} = 0.0085$$

From the stoichiometry of the reaction it is clear that

$$P_{HNO_2\infty} = 2(P_{[N_2O_3]_i} - P_{[N_2O_3]_\infty}) = 0.0126$$

and $P_{H_2O\infty} = P_{H_2O_i} - P_{[N_2O_3]_i} + P_{[N_2O_3]_\infty} = 0.0167$

hence $K = \frac{(0.0126)^2}{0.0085 \times 0.0167} = 1.12$

in fortuitously excellent agreement with the predicted value.

Table I gives experimental conditions, observed values of τ and calculated values of $P_{HNO_2\infty}$ and K for the other runs of this series; the average for the set is 1.16, the range 0.61 to 2.06. This constitutes satisfactory confirmatory evidence concerning the order of magnitude of K .

TABLE I

Frame No.	Flow rate cm ³ /sec.	$P_{D_{1,0}J_i} \times 10^2$	$P_{H_2O_i} \times 10^2$	$P_{HNO_3} \times 10^2$	$\tau \times 10^2$	K
29	8.1	1.80	1.89	1.54	1.7	2.06
31	8.1	1.80	1.89	1.54	2.2	2.06
33	8.1	1.80	1.49	1.12	3.5	1.09
35	8.1	1.80	1.49	1.14	3.8	1.12
38	7.9	1.85	0.96	0.82	5.1	0.85
39	7.8	1.90	.95	.78	4.4	.72
45	7.4	1.43	.98	.78	5.7	.96
46	7.4	1.46	.98	.78	5.7	.96
49	7.3	1.49	1.47	.82	4.4	.61
51	7.1	1.49	2.3	1.26	1.4	1.12
52	7.1	1.48	2.3	1.26	1.4	1.12

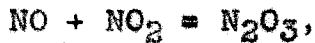
IV. ORDER OF THE REACTION.

A. Characteristics of the rate curve.

In mixtures containing the gases nitric oxide, nitrogen dioxide and water, other substances which may be present at equilibrium include oxygen and the sesquioxide, tetroxide, pentoxide and trioxide of nitrogen as well as the vapors of nitrous and nitric acids. For the equilibrium constant $P_{NO} P_{O_2}^{1/2} / P_{NO_2}$ at 298°C Giauque and Kemp (12) give 7.2×10^{-7} ; for the constant $P_{NO} P_{HNO_3}^2 / P_{NO_2}^3 P_{H_2O}$ Forsythe and Giauque (9) give 1.05×10^{-2} at the same temperature. Since in this study P_{NO} was about unity and P_{NO_2} and P_{H_2O} were of the order of 10^{-2} , the equilibrium concentrations of oxygen and nitric acid vapor are of the order of 10^{-14} and 10^{-5} respectively and can be neglected. Clearly, nitrogen pentoxide and trioxide will also be absent under these conditions. The concentration of

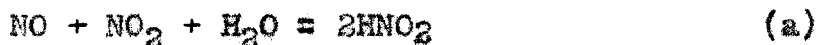
nitrogen tetroxide will also be neglected; this is further discussed below (Section IV-C).

Since it has been shown that there is no lag in establishment of the equilibrium



at least within the limits of observation of the apparatus, it follows that any reaction which proceeds with a measurable velocity in such a system must furnish the end-product HNO_2 .

The two reactions which thus come into consideration are



For the purposes of this investigation, however, it is immaterial which of these reactions is the faster. Indeed, no evidence is furnished concerning this point, as the variables P_{NO_2} , $P_{\text{N}_2\text{O}_3}$, and $P_{[\text{N}_2\text{O}_3]} (= P_{\text{NO}_2} + P_{\text{N}_2\text{O}_3})$ are essentially identical, differing at all times only by a scale factor. In any event, the net reaction can be written



(where the notation $[\text{N}_2\text{O}_3]$ signifies available nitrogen sesquioxide) with the equilibrium constant $K = 1.1$ as discussed in Section III-B. Remembering that $P_{\text{NO}_2} = 1$, the differential rate equation can be expressed by

$$\frac{dx}{k dt} = Y \left[(a - \frac{x}{2})(b - \frac{x}{2}) - \frac{x^2}{K} \right] \quad (1)$$

where x denotes P_{HNO_2} as a function of time t ,

a is the initial value of $P_{[\text{N}_2\text{O}_3]}$,

b is the initial value of $P_{\text{H}_2\text{O}}$,

k is the assumed rate constant of the forward reaction and Y is a factor which may be variable, reflecting any influences which affect forward and reverse reactions equally. The validity of this expression follows if it be assumed that the mechanisms of the forward and reverse reactions in non-equilibrium mixtures at any instant are the same as those of the reactions which balance when equilibrium is reached.

If the factor Y can be expressed as a polynomial in x , or if it is constant, this expression may be integrated by a straightforward method involving partial fractions. If Y is taken to be a constant, corresponding to the obvious hypothesis that collision between suitably activated molecules of N_2O_3 and H_2O is the rate determining step, and if K is assigned the value 4, the integrated curve proves to be of the form

$$x_{\infty} - x = x_{\infty} e^{-mk t} \quad (2)$$

where x_{∞} denotes the equilibrium pressure of HNO_3 and m is a numerical factor independent of x and t .

Thus under these conditions a plot of $\log(x_{\infty} - x)$ vs. t gives a straight line whose slope is proportional to m ; a convenient measure of this slope is the half-time, which is constant and inversely proportional to m .

It can be shown that if K is of the order of magnitude of 4 the same relations hold approximately, and that this is also true even if Y is variable, as long as its magnitude does not change greatly during the course of reaction. In

agreement with these considerations it was found that semi-log plots of the individual runs did indeed furnish approximately straight lines, and that the slope of such lines depended upon the initial concentrations of the reagents much more sensitively than did the curvature. (See Figure 5, in which curves a and b correspond to the photograph, Figures 4a and 4b, respectively.) The procedure adopted, therefore, was to plot the data in terms of displacement from equilibrium vs. time on semi-log paper, draw the most plausible straight line through the points, and measure the apparent half-time from this straight line, the order of reaction was then tested by investigating the dependence of this apparent half-time on the initial concentrations.

B. Derivation of Order Tests.

Rearranging (1) leads to the equation

$$kdt = \frac{dx}{Y[(a-\frac{x}{2})(b-\frac{x}{2}) - \frac{x^2}{K}]} \quad (3)$$

which can be integrated exactly with the aid of Pierce's integral 68. Utilizing for convenience the substitutions

$$R = \frac{4-K}{K} \quad (4)$$

and $F = \sqrt{a^2 + (4R+2)ab + b^2} = \sqrt{(a-b)^2 + 16ab/K} \quad (5)$

and applying the initial condition, $x = 0$ when $t = 0$, the result is

$$kt = \frac{4}{FY} \left(\tanh^{-1} \frac{R_x + a + b}{F} - \tanh^{-1} \frac{a + b}{F} \right); \quad (6)$$

Solving for x gives

$$x = R^{-1} \left[-(a+b) + F \tanh \left(\frac{kt}{4} FY + \tanh^{-1} \frac{a+b}{F} \right) \right]. \quad (7)$$

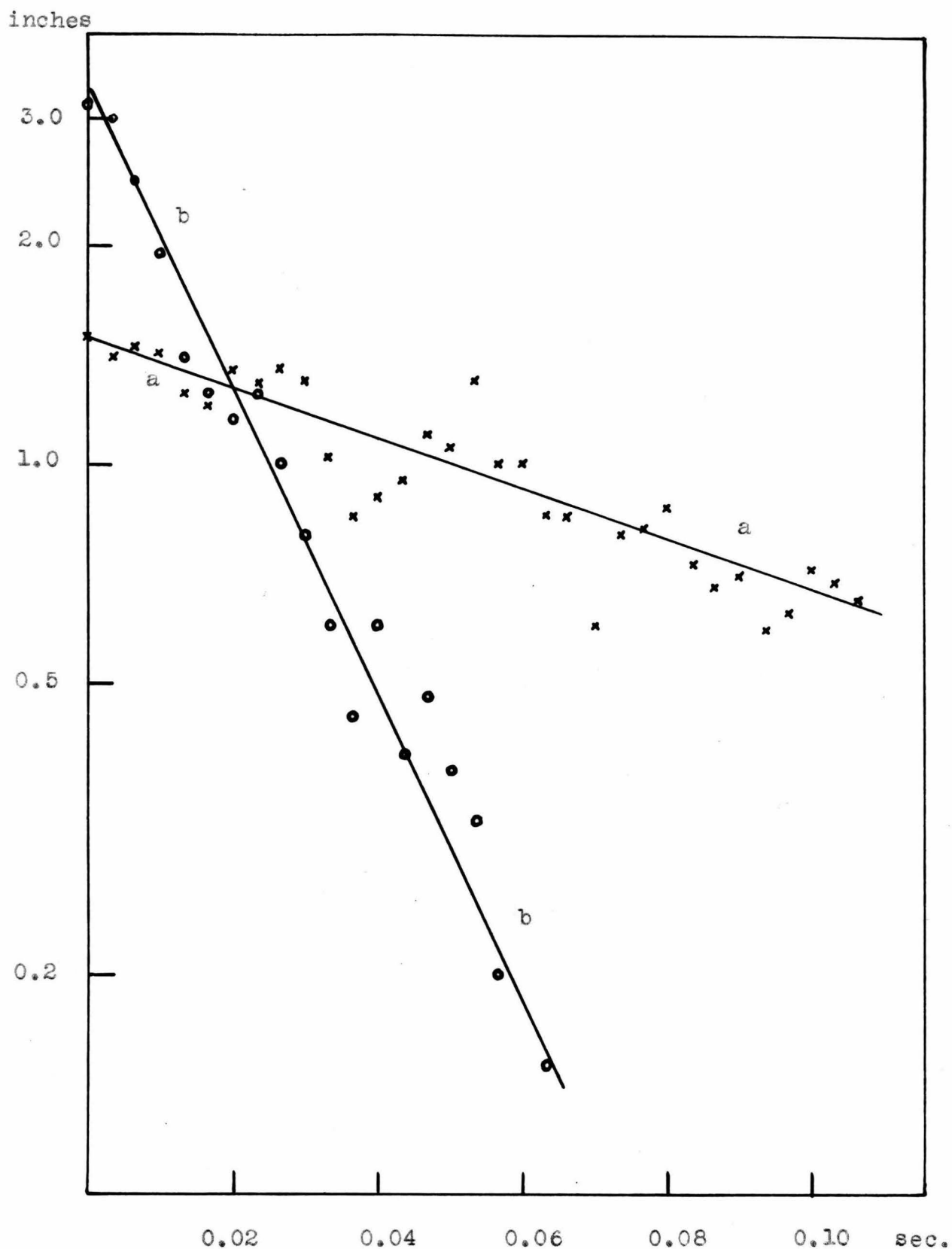


Figure 5. Displacement from equilibrium vs. time (semi-log plot)
Curve a, Run IV-59, corresponding to Figure 4a
Curve b, Run IV-52, corresponding to Figure 4b

As t increases without limit, x_∞ approaches x_∞ , and (7) becomes

$$x = \frac{F - a - b}{R} \quad (8)$$

combining this with (7) one finds

$$x_\infty - x = \frac{F}{R} \left[1 - \tanh \left(\frac{kt}{4} FY + \tanh^{-1} \frac{a+b}{F} \right) \right]. \quad (9)$$

The slope of the curve representing $x_\infty - x$ vs kt on a semi-log plot is given by

$$\begin{aligned} \frac{d \ln(x_\infty - x)}{d kt} &= \frac{d(x_\infty - x)}{(x_\infty - x) k dt} \\ &= - \frac{FY}{4} \frac{\operatorname{sech}^2 \left(\frac{kt}{4} FY + \tanh^{-1} \frac{a+b}{F} \right)}{\left[1 - \tanh \left(\frac{kt}{4} FY + \tanh^{-1} \frac{a+b}{F} \right) \right]}, \end{aligned}$$

or, since $\operatorname{sech}^2 \theta = 1 - \tanh^2 \theta$,

$$\frac{d \ln(x_\infty - x)}{k dt} = - \frac{FY}{4} \left[1 + \tanh \left(\frac{kt}{4} FY + \tanh^{-1} \frac{a+b}{F} \right) \right]. \quad (10)$$

This increases monotonically with time, the ratio of final value to initial value being expressible as

$$\eta = 2F/(F+a+b) \quad (11)$$

It is not difficult to show that this ratio is a maximum when a and b are taken equal, corresponding to the value

$$\eta_{\max} = 4/(2+\sqrt{K}). \quad (12)$$

Assuming a value of K not less than 1, η would be not greater than $4/3$. Examining the shape of the appropriate hyperbolic tangent curve, one finds that the major part of this variation in slope occurs during the first half-time of the reaction. Thus a set of data which accurately followed such a law could

be approximately represented (on the semi-log plot) by a straight line asymptotic to the curve.

Another case of interest is that Y may be proportional to the concentration of one of the reactants. If $Y = b - \frac{x}{2}$, equation (3) may be conveniently rearranged into the form

$$\frac{1}{8} R k dt = \frac{dx}{(A-x)(B+x)(C-x)}, \quad (13)$$

where A , B , and C are the magnitudes of the roots of the polynomial in the denominator. Specifically,

$$A = R^{-1}(F-a-b) = x_{\infty}, \quad (14)$$

$$B = R^{-1}(F+a+b) = x_{\infty} + 2(a+b)/R \quad (15)$$

$$C = 2b \quad (16)$$

Re-expressing (13) in terms of partial fractions, it becomes

$$\frac{1}{8} R k dt = \frac{dx}{(A+B)(C-A)(A-x)} + \frac{dx}{(B+A)(B+C)(B+x)} - \frac{dx}{(C-A)(B+C)(C-x)} \quad (17)$$

or, remembering that $dx = d(B+x) = -d(A-x) = -d(C-x)$,

$$\frac{1}{8} R k dt = -\frac{d \ln(1 - \frac{x}{A})}{(A+B)(C-A)} + \frac{d \ln(1 + \frac{x}{B})}{(B+A)(B+C)} + \frac{d \ln(1 - \frac{x}{C})}{(C-A)(B+C)}. \quad (18)$$

In view of (14), therefore,

$$\frac{d \ln(x_{\infty} - x)}{k dt} = -\frac{1}{8} R (A+B)(C-A) + \frac{(C-A)}{(B+C)} \frac{d \ln(1 + \frac{x}{B})}{k dt} + \frac{(A+B)}{(B+C)} \frac{d \ln(1 - \frac{x}{C})}{k dt}. \quad (19)$$

As t increases without limit the last two terms of (19) approach zero, so that using (14), (15), and (16) the asymptotic slope is found to be

$$\frac{d \ln(x_{\infty} - x)}{k dt} \approx -\frac{F}{2} \left(b - \frac{x_{\infty}}{2} \right). \quad (20)$$

It is interesting to note that (19) is formally equivalent to

the asymptotic approximation

$$\frac{d \ln (x_0 - x)}{k dt} \approx - \frac{FY}{2} \quad (21)$$

derivable from (10).

From the preceding discussion it will be clear that the apparent half-time to be used in testing the dependence of rate upon concentrations should be obtained from a line asymptotic to the data rather than one passing through the data themselves. Because of the relatively large standard error of the individual points, however, this was not practical and the method outlined in Section A was followed. In this manner an apparent half-time τ was found for each individual run, and combining this with the recorded concentrations the quantities τF , $\tau F(b - \frac{x_0}{2})$, and others were calculated. The assembled values were examined for their constancy particularly with reference to the existence of any trends relating the calculated values to the initial concentrations or the ratio of initial concentrations.

C. Discussion of the approximations.

For purposes of discussion, three principal approximations may be recognized: (i) the assumption of linear response of the detecting and recording system; (ii) neglect of complicating factors in interpreting the composition of the reacting mixture; (iii) uncertainty in the determination of the asymptotic half-time for each run. The first assumption was checked by calibration, as discussed in Section II-G; the errors due to non-linearity of this sort in all probability would affect observed amplitude differences by less than

5 per cent. A systematic error is indeed introduced in assuming that the quantity $x_{\infty} - x$ is linearly dependent on the distance of the points on the tracing from the equilibrium position, since the intensity of transmitted light is an exponential function of the concentration. This may be illustrated by a calculation, using the data of run IV-52 (which has been previously cited in Section III-B). From the photograph the steady state amplitude and equilibrium amplitude were 23.0 and 26.0 inches, respectively, corresponding to $P_{[N_2O_3]}$ of 0.0119 and 0.0085 (calculated from equation III-1). A point giving the exactly intermediate amplitude 24.5 inches would correspond to $P_{[N_2O_3]} = 0.0103$, while the linear approximation would give instead 0.0102; the half-time calculated on this basis would be shorter than the true value by 6 per cent. This example is an extreme one because the amplitude change involved is large. In most runs the error caused by this procedure would be certainly less than 5 per cent.

Complicating factors in determining the composition of the reacting mixtures are the presence of nitrogen tetroxide, the change of pressure of nitric oxide as a result of reaction, and the fact that the gas mixture at the exit end of the light path is older than that near the inlet. At 25°C, the dissociation constant of N_2O_4 is 0.14 atm., from which it may be shown that $P_{N_2O_4} = 7P_{NO_2}^2 = 3P_{[N_2O_3]}^2$; i.e., the pressure of N_2O_4 ranges up to about 10 per cent of the total available N_2O_3 , being in most cases nearer to 5 per cent. If

N_2O_4 is a non-participating molecular species it should affect the half-time by providing a reservoir of $[N_2O_3]$ which would not be detected by absorption of light. This effect should be comparable in magnitude but opposite in sign to that of the systematic error discussed in the previous paragraph, providing some compensation in this respect. The change in P_{N_2} due to its disappearance in the reaction is of the order of one per cent or less and may legitimately be neglected. Non-uniformity of the gas mixture in the light path is not particularly disturbing because of the fortunate circumstance that the course of the reaction is approximately exponential, so that the half-time is roughly the same for all parts of the system and consequently is given by that of the integrated system. At any rate, the maximum age difference to be considered was about one hundredth of a second, so that no important effect would be expected except perhaps for those runs giving the very shortest half-times.

Uncertainty in the determination of the half-time is due to two principal causes, namely uncertainty in determining the proper slope on the semi-log plot, due to scatter of the individual points, and uncertainty in the determination of the value $x_\infty - x$ for the individual points due to drift of the pattern. As may be seen by examining Figure 5, the points which are useful in the semi-log plot range over a period of only two or three half-times, so that the half-time estimated is likely to fall between the asymptotic value and the initial

value. The quantity η , defined as the ratio of final to initial slope of the theoretical curve on the semi-log plot (i.e., $[d \ln(x_{\infty} - x)/dt]_{\infty} / [d \ln(x_{\infty} - x)/dt]_i$;) has already been shown (Section IV-B) to vary between 1 and 1.3 on the assumption of a second order rate law. A similar treatment shows that if a third order rate law is assumed, η may vary over somewhat wider limits. Setting $x = 0$ in equation (17) and rearranging,

$$\frac{dx}{dt} = \left[-\frac{1}{A} - \frac{C-A}{B(B+C)} + \frac{A+B}{C(B+C)} \right] = -\frac{1}{8} R(A+B)(C-A); \quad (22)$$

hence $\left[\frac{d \ln(x_{\infty} - x)}{k dt} \right]_i = -\frac{dx}{A k dt} = -\frac{1}{8} \frac{R B C (A+B)(C-A)(B+C)}{B C (B+C) + C A (C-A) - A B (A+B)} \quad (23)$

But from equation (19), since the last two terms vanish at

$$\left[\frac{d \ln(x_{\infty} - x)}{k dt} \right]_{\infty} = -\frac{1}{8} R(A+B)(C-A), \quad (24)$$

giving

$$\eta = 1 + \frac{C A (C-A) - A B (A+B)}{B C (B+C)} \quad (25)$$

To illustrate the magnitude of η , results of calculation for a few typical cases are shown in Table II.

TABLE II

$a \times 10^2$	$b \times 10^2$	$f \times 10^2$	$A (= x_{\infty}) \times 10^2$	$B \times 10^2$	$C (= 2b) \times 10^2$	η
0.5	2.5	4.7	0.65	2.9	5.0	1.06
1.5	2.3	7.1	1.25	4.1	4.6	0.95
1.5	1.5	5.7	1.02	3.3	3.0	0.87
2.5	1.0	6.2	1.03	3.7	2.0	0.62

The values of γ obtained in examples 1 and 4 represent the extremes to be encountered in this study; 2 and 3 are more typical values (the data in line 2 correspond to those of run IV-52, already cited in Section III-B). Since the slope changes most rapidly during the first half-time of the reaction it is likely that the slope of the line chosen will differ from the asymptotic slope by considerably less than is indicated by the factor γ . The average error from this cause is probably of the order of 10 per cent or less, except possibly in a few cases where the ratio a/b is unusually high.

The drift of the pattern following its sudden displacement presents a less easily handled problem. This effect is clearly evident on those photographs in which the half-time is very short; the observed displacement rises sharply to a maximum, then falls off more slowly. If it be assumed as a first approximation that this drift also follows an exponential law, its half-time may be estimated as about 0.10 to 0.15 seconds. An attempt was made to estimate the magnitude of the uncertainty from this cause in the following way: on tracings derived from several runs of very short half-time, the sloping envelope of the latter portion was extrapolated linearly and the half-time was determined from a semi-log plot representing the data as displacement from this line. This resulted in an increase of 20 to 25 per cent for half-times estimated by the ordinary method as less than 0.02 seconds. Since this process could not be applied in most cases, the trend of the discrepancy with increasing half-time could not be determined,

but it seems likely that as the prominence of the maximum lessens the disturbance of the measured half-time does also.

D. The results.

Listed in Table III are the temperature, composition, and total flow rate for each experiment, together with the half-time τ (determined as explained above) and the products τF and $\tau F(b - \frac{x_\infty}{2})$ which serve to test respectively the second and third order hypotheses. Figures 6 and 7 present these results graphically. In Figure 6a, where the values of τF are plotted against b , the initial pressure of water vapor, there can be observed a distinct trend in the sense of inverse variation, whereas in Figure 6b a comparable plot of $\tau F(b - \frac{x_\infty}{2})$ vs. b displays no such trend. In figures 7a and 7b respectively, the same products are plotted against α , the initial value of $P_{[N_2O_3]}$, the "available" N_2O_3 . No trends are evident in these charts, but it can be seen that the points in Figure 7a are more widely scattered than those in 7b, with respect to both the extreme range and the range of more frequent values. Thus in 7a, the ratio between highest and lowest values is about 10, while in 7b it is near 4; similarly in 7a, the ratio between values excluding the highest and lowest five per cent of the points is 3.5, while in 7b it is 1.9.

These considerations indicate that of the hypotheses tested the third order law corresponding to Equation IV-3 with $Y = P_{H_2O}$ is the most satisfactory; i.e., the reaction may be considered first order with respect to N_2O_3 and second order

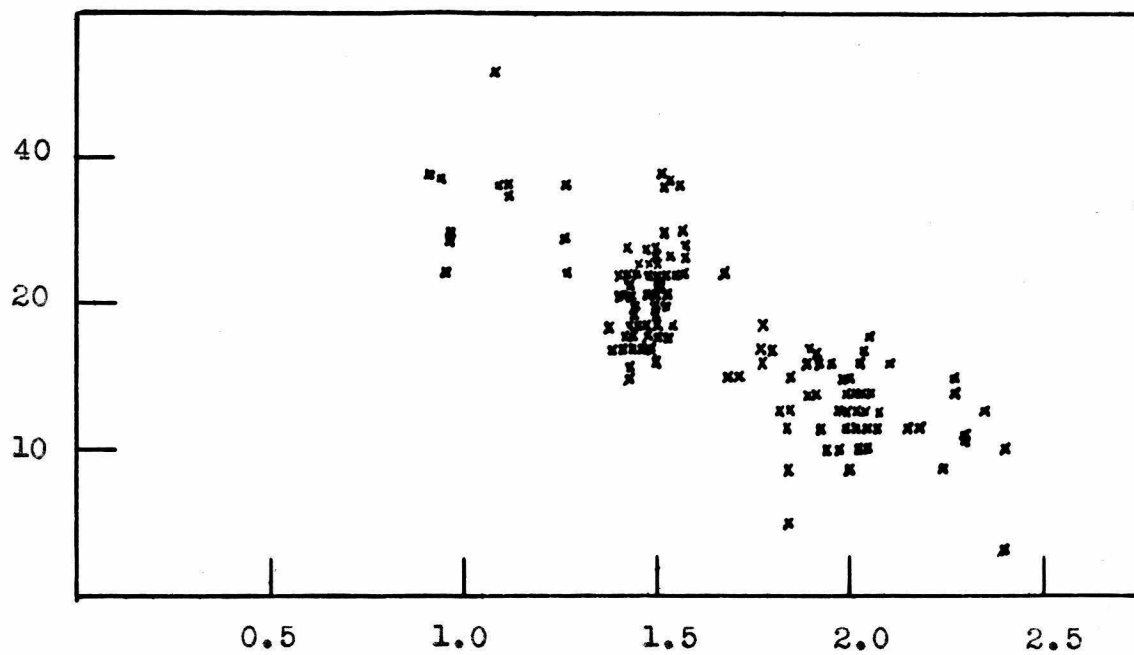


Figure 6a. $\tau F \times 10^4$ vs. $P_{H_2O} \times 10^2$

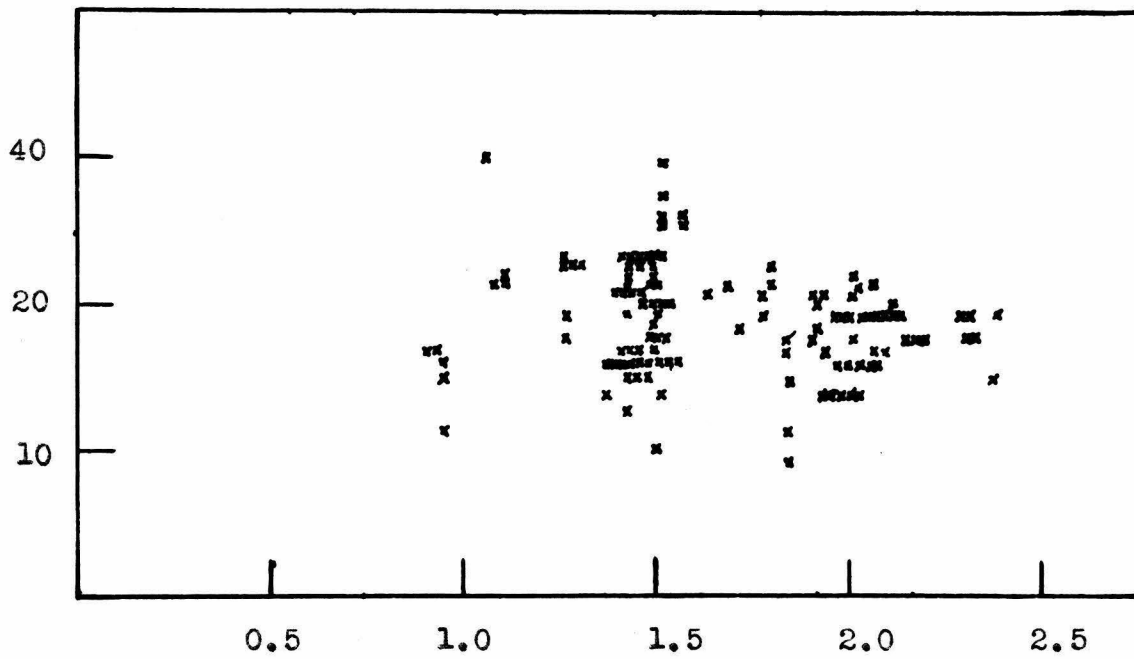


Figure 6b. $\tau F (b - \frac{x_{so}}{\lambda}) \times 10^6$ vs. $P_{H_2O} \times 10^2$

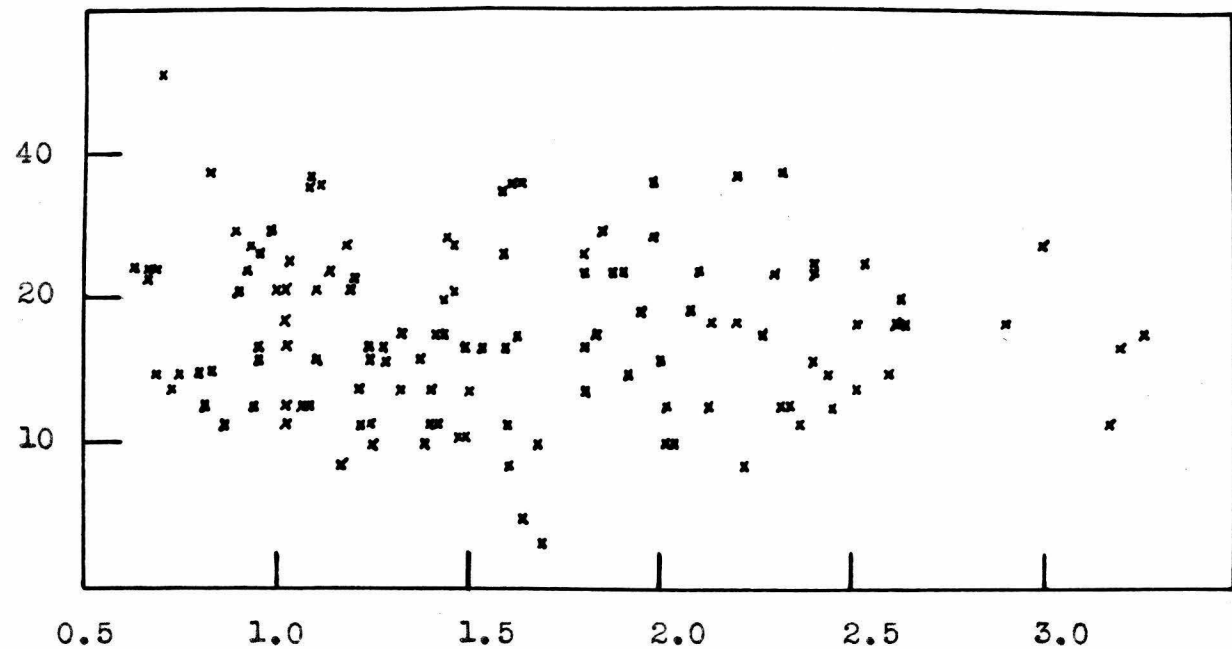


Figure 7a. $\tau F \times 10^4$ vs. $P_{[N_2O_3]i} \times 10^2$

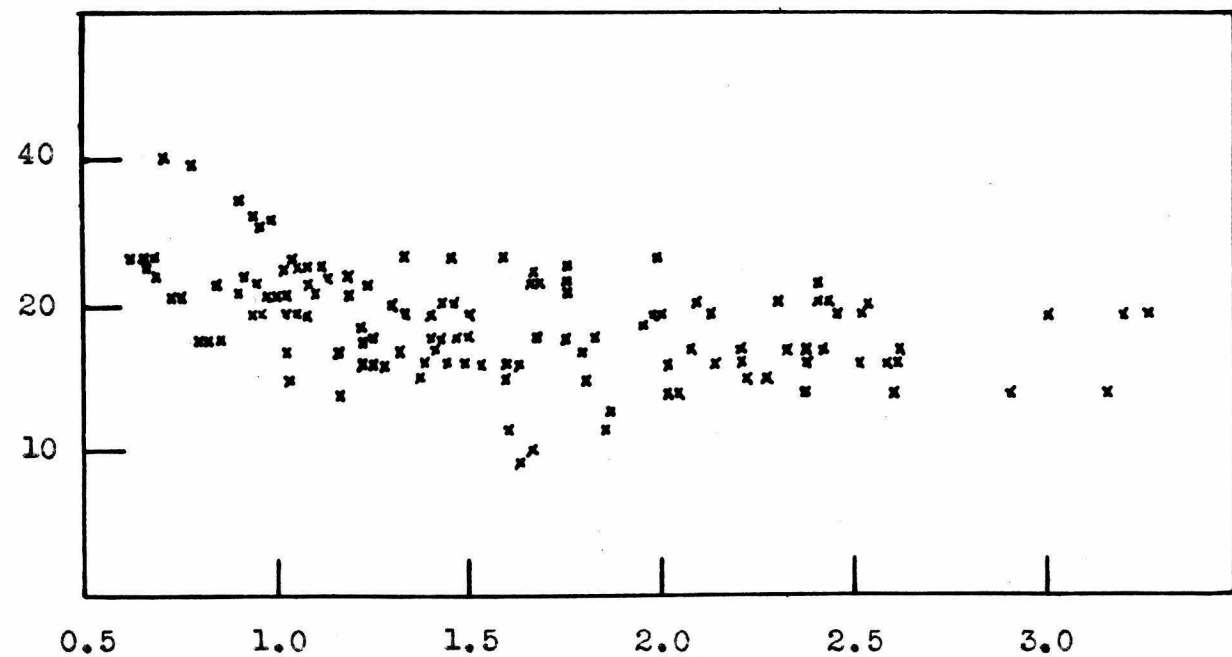


Figure 7b. $\tau F(b - \frac{x_{oo}}{2}) \times 10^6$ vs. $P_{[N_2O_3]i} \times 10^2$

with respect to H_2O . The reverse reaction must, for consistency, likewise be assumed to be third order, its rate depending on the first power of water vapor pressure and the square of the pressure of nitrous acid vapor.

Table IV presents the data concerning the tests on dilution of $NO-NO_2$ mixtures with N_2 . A separate blank was taken for each run; the photographs obtained showed no evidence of lag in attaining equilibrium.

TABLE III

Film no.	T $^{\circ}C$	Flow Rate $cm^3/sec.$	$P_{[N_2O_3]_i} \times 10^2$ atm	$P_{H_2O_i} \times 10^2$ atm	$\frac{P_{[N_2O_3]_i}}{P_{H_2O_i}}$	F $\times 10^2$ atm	$\tau \times 10^2$ sec	$\tau F \times 10^4$	$\tau F(b - \frac{x^{\infty}}{2}) \times 10^6$
I-1	25	9.5	1.48	1.43	1.03	5.67	2.8	16	15
2	25	9.4	1.53	1.42	1.08	5.92	2.7	16	15
3	25	9.2	1.59	1.42	1.12	6.02	2.7	17	15
5	25	8.9	1.24	1.43	0.87	5.35	3.0	16	15
6	25	8.8	1.28	1.42	.90	5.25	3.0	16	15
7	25	8.7	1.32	1.43	.92	5.51	3.1	17	16
8	25	8.6	1.37	1.42	.97	5.60	2.7	15	14
9	25	8.6	0.90	1.42	.63	4.57	4.6	21	21
10	25	8.5	.92	1.43	.64	4.64	5.0	23	23
11	25	8.2	1.00	1.42	.71	4.81	4.4	21	21
12	25	8.2	1.00	1.42	.71	4.81	4.3	21	21
13	25	8.0	0.63	1.42	.44	3.88	6.0	23	25
14	25	8.0	.66	1.42	.46	3.96	5.6	22	24
15	25	7.8	.67	1.41	.47	3.96	5.7	23	25
16	25	7.8	.69	1.41	.49	3.89	5.9	23	25
21	25	7.0	2.32	2.07	1.12	8.86	1.4	12	16
22	25	7.0	2.33	1.99	1.17	8.67	1.4	12	15
23	25	6.9	2.36	1.93	1.22	8.60	1.3	11	13
24	25	6.8	2.44	1.92	1.27	8.70	1.6	14	16
26	25	9.6	1.38	2.05	0.68	6.80	1.5	10	15
27	25	9.6	1.41	2.05	.69	6.86	1.6	11	16
28	25	9.2	1.50	2.05	.73	7.07	1.8	13	19
29	25	8.9	1.60	2.02	.79	7.23	1.5	11	15
30	25	8.7	1.25	2.03	.62	6.45	1.6	10	15
31	25	8.6	1.24	2.03	.61	6.42	2.3	15	22

TABLE III (CONT.)

Film no.	T °C	Flow Rate cm ³ /sec	$P_{[N_2O_4]} \times 10^2$ atm	$P_{H_2O} \times 10^2$ atm	$\frac{P_{[N_2O_4]}}{P_{H_2O}}$	$F \times 10^2$ atm	$\tau \times 10^2$ sec	$\tau F \times 10^4$	$\tau F(b - \frac{x_0}{2}) \times 10^6$
I-32	25	8.6	1.32	2.03	0.65	6.61	1.9	13	19
	33	8.3	1.40	2.03	.69	6.80	1.9	13	19
	34	8.2	0.94	2.02	.46	5.63	2.2	12	19
	35	8.0	1.06	2.00	.53	5.92	2.1	12	19
	36	8.0	1.08	2.00	.54	5.97	2.0	12	19
	37	7.7	1.16	2.00	.58	6.18	1.4	9	13
	38	7.4	0.69	2.00	.34	4.90	2.8	14	23
	39	7.4	.73	2.00	.37	5.01	2.6	13	21
	40	7.0	.84	1.99	.42	5.31	2.6	14	22
	41	7.0	.86	1.99	.43	5.37	2.1	11	17
42	25	7.1	1.52	1.02	1.49	5.02	6.8		
	47	6.7	1.08	1.04	1.04	4.26	8.5	36	24
	48	6.6	1.08	1.06	1.02	4.35	8.1	35	24
	49	6.5	1.12	1.03	1.09	4.32	8.0	35	24
	66	9.7	1.03	1.44	0.71	4.92	4.8	24	25
	67	9.4	1.13	1.42	.80	5.08	4.6	23	23
	68	9.1	1.19	1.44	.83	5.16	4.1	21	21
II-3	24	6.8	1.03	1.50	0.69	4.90	3.6	18	19
	4	6.8	1.09	1.50	.73	5.20	3.6	21	22
	5	6.7	1.19	1.50	.79	5.40	4.1	22	23
	6	6.4	1.68	2.40	.70	7.50	0.9	6	10
	16	7.1	1.39	2.16	.64	7.00	1.6	11	17
	17	7.3	1.23	2.16	.57	6.70	1.6	11	17
	18	7.2	1.25	2.15	.58	6.70	1.7	11	17
	19	6.9	1.10	1.90	.58	5.90	2.5	15	21
	20	6.9	1.22	1.90	.64	6.20	2.1	13	18
	21	6.9	1.29	1.90	.68	6.40	2.4	15	20
	22	6.7	0.89	1.56	.57	4.80	5.8	28	33
23	24	6.8	.93	1.57	.59	5.00	5.2	26	30
	24	6.7	.95	1.58	.60	5.00	5.0	25	29
	25	6.3	.70	1.07	.70	3.00	20.	60	40
	29	6.0	2.12	2.36	.90	9.00	1.3	12	19
	30	5.9	2.22	2.34	.95	9.10	1.0	9	14
	32	5.7	2.00	1.95	1.03	7.90	1.9	15	19
	33	5.7	2.04	1.95	1.05	8.00	1.3	10	13
	34	5.4	2.02	1.95	1.04	8.00	1.2	10	13
	35	5.4	2.01	1.95	1.03	7.90	1.5	12	15
	36	5.3	1.43	1.49	0.96	5.80	2.9	17	17
	37	5.3	1.43	1.49	.96	5.80	3.5	20	20
	38	5.3	1.46	1.49	.98	5.90	3.5	21	20
42	24	4.8	3.27	2.06	1.59	10.50	1.6	17	19
	43	4.6	3.16	2.01	1.57	10.20	1.1	11	13

TABLE III (CONT.)

Film no.	T °C	Flow Rate cm ³ /sec	P _{IN,O₂} × 10 ² atm	P _{H₂O} × 10 ² atm	P _{IN,O₂} / P _{H₂O}	F × 10 ² atm	τ × 10 ² sec	τF × 10 ⁴	τF(b - x _∞) × 10 ⁶
II-44									
	24	4.6	2.57	1.49	1.73	8.00	2.3	18	15
	45	4.6	2.57	1.49	1.73	8.00	2.3	18	15
	46	6.7	1.83	1.50	1.22	6.60	2.6	17	16
	47	6.5	1.95	1.50	1.30	6.80	2.8	19	18
	48	6.4	2.54	1.51	1.68	7.90	3.1	24	20
	49	6.2	2.51	1.50	1.67	7.80	2.3	18	15
	50	6.1	2.60	1.51	1.72	7.90	1.9	15	13
	51	6.0	1.87	1.26	1.48	6.20	5.3	23	17
	52	5.9	1.98	1.26	1.57	6.30	4.2	27	19
II-53									
	24	5.9	1.98	1.26	1.57	6.30	5.5	35	25
	55	5.5	1.65	1.09	1.51	5.30	6.5	35	22
	56	5.5	1.66	1.11	1.49	5.40	6.5	35	23
	57	5.5	1.67	1.11	1.51	5.40	6.3	34	22
	61	5.0	0.94	1.76	0.53	5.20	2.9	15	19
	62	5.0	.95	1.79	.53	5.30	3.0	16	22
	63	4.9	1.03	1.77	.58	5.40	2.9	16	21
	64	4.9	1.03	1.77	.58	5.40	3.3	18	24
III-2									
	24	6.9	1.91	1.42	1.34	6.70	2.1	14	12
	4	6.8	2.08	1.43	1.45	6.90	2.7	19	16
	6	6.8	2.27	1.43	1.59	7.20	2.4	17	14
	8	6.4	2.62	1.43	1.83	7.70	2.6	20	16
	11	6.0	2.13	1.45	1.47	7.00	2.5	25	15
	12	6.0	2.20	0.94	2.3	5.90	6.0	36	16
	13	5.9	2.52	.91	2.5	6.00	6.3	37	16
	18	5.4	2.45	2.27	1.08	9.60	1.4	13	19
	19	5.4	2.52	2.27	1.11	9.80	1.4	14	18
IV-38									
	23	5.4	2.9	1.58	2.1	7.50	2.4	18	13
	23	3.3	3.0	1.43	2.1	8.50	3.1	26	19
	27	3.1	3.2	2.04	1.6	10.50	1.6	16	19
	29	8.1	1.80	1.89	0.95	7.40	1.7	13	17
	51	8.1	1.80	1.89	0.95	7.40	2.2	16	21
	33	8.1	1.80	1.49	1.21	6.60	3.5	23	22
	35	8.1	1.80	1.49	1.21	6.60	3.8	25	24
	38	7.9	1.85	0.96	1.9	5.43	5.1	28	14
	39	7.8	1.90	.95	2.0	5.48	4.4	23	11
IV-43									
	24	7.5	1.44	.96	1.50	4.75	5.7	27	15
	45	7.4	1.43	.98	1.46	4.80	5.7	27	15
	46	7.4	1.46	.98	1.49	4.85	5.7	27	15
	48	7.4	1.43	1.50	0.95	5.90	3.5	17	17
	49	7.3	1.45	1.47	.99	5.87	4.4	26	25
	51	7.1	1.49	2.3	.65	7.50	1.4	11	17
	53	7.1	1.48	2.3	.65	7.47	1.4	11	17

TABLE III (CONT.)

Film No.	T °C	Flow Rate cm ³ /sec	$P_{[N_2O_3]_i} \times 10^2$ atm	$P_{H_2O_i} \times 10^2$ atm	$\frac{P_{[N_2O_3]_i}}{P_{H_2O_i}}$	$F \times 10^2$ atm	$\tau \times 10^2$ sec	$\tau F \times 10^4$	$\tau F(b - \frac{x_0}{2}) \times 10^6$
IV-54	24	6.9	1.58	1.52	1.04	6.23	4.0	25	25
	55	6.8	1.33	1.50	0.89	5.70	4.6	26	25
	56	6.7	0.99	1.52	.65	4.95	5.6	28	30
	59	6.6	.78	1.51	.51	4.43	8.3	37	39
	65	6.0	2.3	1.50	1.53	7.52	3.1	23	20
	66	5.9	2.4	2.1	1.14	9.05	1.7	15	20
	67	5.9	2.4	1.67	1.43	8.10	2.8	23	22
	V-19	23	6.5	1.60	1.83	0.88	6.90	1.3	9
	21	6.5	1.63	1.83	.89	6.90	1.0	7	10
	34	6.5	0.81	1.83	.44	4.80	2.4	12	17
	30	7.5	.75	1.63	.41	4.50	3.0	14	21
	31	7.2	.79	1.70	.46	4.70	2.9	14	18
	43	7.6	1.03	1.83	.56	5.60	2.0	11	14
	45	7.6	1.03	1.83	.56	5.60	2.2	12	16
VI-14	24	4.0	2.1	1.45	1.45	7.00	3.3	23	20
	17	3.8	2.2	1.45	1.52	7.20	2.5	18	15
	23	3.6	2.4	1.45	1.65	7.50	3.2	24	20

TABLE IV

	Flow rate cm ³ /sec			T °C	Dilution Ratio N ₂ /NO
	N ₂	NO	O ₂		
1	4.1	1.8	0.031	23	2.3
2	4.1	1.7	.028	23	2.4
3	7.1	1.6	.027	23	4.5
4	3.3	1.6	.039	23	3.1

As a result of this observation, a lower limit may be estimated for the rate of dissociation of nitrogen sesquioxide. If the rate constant and equilibrium constant for the dissociation are k_c and K_c respectively, the differential rate equation

may be written

$$-\frac{dP_{N_2O_3}}{dt} = k_c (P_{N_2O_3} - \frac{1}{K_c} P_{NO} P_{NO_2}). \quad (1)$$

Setting $a' = P_{N_2O_3}$ and $a'' = P_{NO_2}$, so that $a' + a'' = P_{[N_2O_3]} = a$, (1) is also expressible as

$$\begin{aligned} -\frac{da'}{dt} &= k_c (a' - a'' \frac{P_{NO}}{K_c}) \\ &= k_c [a' (1 - \frac{P_{NO}}{K_c}) - \frac{a'' P_{NO}}{K_c}]. \end{aligned} \quad (2)$$

This is readily integrated to give the exponential rate law

$$a' = \frac{a P_{NO}}{K_c - P_{NO}} + e^{-(1 - \frac{P_{NO}}{K_c}) k_c t} \left(a' - \frac{a P_{NO}}{K_c - P_{NO}} \right), \quad (3)$$

which leads to the half-time

$$\tau_c = \frac{K_c \ln 2}{k_c (K_c - P_{NO})}, \quad (4)$$

P_{NO} being considered constant during the course of dissociation.

Since the highest flow rate used in these tests was nearly $9 \text{cm}^3/\text{sec}$. and the volume between the point of dilution and the point of observation about 0.1cm^3 , it may reasonably be assumed that the lapse of at least two half-times required not more than 0.01sec . In the same run, P_{NO} was less than 0.2 ; K_c is 2.1 (see Section III-A). Substitution of these values in (4) provides the estimate $k_c < 150 \text{ sec}^{-1}$.

V. CONCLUSIONS

A. The rate constant.

Assuming for the formation of HNO_2 the rate law

$$\frac{dx}{kdt} = (b - \frac{x}{2}) \left[(a - \frac{x}{2})(b - \frac{x}{2}) - \frac{x^2}{K} \right]$$

which has been discussed in Part IV, the rate constant k may be calculated from the relation

$$k = \frac{2 \ln 2}{\tau F (b - \frac{x_\infty}{2})}$$

where the denominator is the product represented in figures 6b and 7b. The median value of this product from all the experiments is 1.9×10^{-5} , which, when substituted, leads to the result at 23 to 25°C with $P_{\text{NO}} = 1 \text{ atm.}$, $k = 7.3 \times 10^4 \text{ atm}^{-2} \text{ sec}^{-1}$ or $\log k = 4.86$ with a probable error of 0.09, corresponding to a factor of 1.2.

On the same basis, treating the forward and reverse processes separately, one finds

$$-\frac{dP_{[\text{NO}_2]}}{dt} = k' P_{[\text{NO}_2]} P_{\text{H}_2\text{O}}^2,$$

$$k' = \frac{1}{2} k = 3.7 \times 10^4 \text{ atm}^{-2} \text{ sec}^{-1}$$

$$= 2.2 \times 10^{-1} \text{ mole}^{-2} \text{ sec}^{-1}$$

or if the assumption be made that the reacting species is N_2O_3 ,

$$-\frac{dP_{[\text{NO}_2]}}{dt} = k'' P_{\text{N}_2\text{O}_3} P_{\text{H}_2\text{O}}^2$$

and since $P_{[\text{NO}_2]} = 3.1 P_{\text{N}_2\text{O}_3}$ (Section III-B),

$$k'' = \frac{3.1 k}{2} = 1.1 \times 10^5 \text{ atm}^{-2} \text{ sec}^{-1}$$
$$= 6.8 \times 10^7 \text{ l}^2 \text{ moles}^{-2} \text{ sec}^{-1}$$

Finally, for the reverse reaction,

$$-\frac{dP_{HNO_2}}{dt} = k''' P_{HNO_2}^2 P_{H_2O}$$

$$k''' = k/K;$$

taking $K = 1.1$ (Section III-B),

$$k''' = 6.6 \times 10^4 \text{ atm}^{-2} \text{ sec}^{-1}$$
$$= 4.0 \times 10^7 \text{ l}^2 \text{ moles}^{-2} \text{ sec}^{-1}$$

It is clear, of course, that the values here given can apply only to the assumed third order law. If one should choose rather to ignore the trend of the results with water vapor pressure (discusses in Section IV-D) and apply the second order law

$$+\frac{dP_{HNO_2}}{k dt} = (a - \frac{x}{2})(b - \frac{x}{2}) - \frac{x^2}{K},$$

the corresponding values of k , k' , k'' , and k''' would each be reduced from those given above by a factor of very nearly 100 atm^{-1} or 2500 l/mole .

B. Comparison with kinetic theory.

Since the rate of reaction proves to be very high in spite of the rather small concentrations of the reactants, it is of interest to determine whether the simple kinetic theory predicts a sufficiently high rate of triple collisions to account for the observations. For a typical mixture in which the pressures of water vapor and of available N_2O_3 were both

0.015 atm., the required collision rate at 25°C would be

$$Z_3 = \frac{N}{V} \frac{dP_{[N_2O_3]}}{dt} = \frac{N}{V} k' P_{[N_2O_3]} P_{H_2O}^2 = 3 \times 10^{18} \text{ cm}^{-3} \text{ sec}^{-1}$$

(N represents Avogadro's number and V the molar volume).

The number of collisions to be expected may be estimated, following Hinshelwood (13), in the following manner. The rate of binary collisions between molecules of different species is given by

$$Z_2 = n_A n_B \sigma_{AB}^2 \left(\frac{8\pi RT}{\mu} \right)^{1/2}$$

where n_A and n_B are the numbers of molecules of the two kinds per cubic centimeter, σ_{AB} is the mean of the molecular diameters and μ is the reduced molecular weight of the pair (i.e., $\frac{1}{\mu} = \frac{1}{M_A} + \frac{1}{M_B}$). R is the gas constant ($= 8.3 \times 10^7$ c.g.s units per mole) and T the absolute temperature in degrees R. Under the circumstances cited above, $n_{[N_2O_3]}$ and n_{H_2O} would each be 4.0×10^{17} with $n_{N_2O_3} = 1.3 \times 10^{17}$. In the absence of accurate data regarding the molecular diameter of N_2O_3 , we may take 4×10^{-8} cm. as a reasonable value for σ_{AB} ; μ for $N_2O_3 + H_2O$ is 14.7. These substitutions lead to the result $Z_2 = 1.7 \times 10^{24}$ per sec.

As an approximation, the ratio of the number of ternary collisions to the number of binary collisions may be taken to be the same as the ratio of the diameter of the third molecule to the mean free path for that species. The mean free path of water molecules at 0.015 atm. and 25°C, assuming $\sigma_{H_2O} = 3 \times 10^{-8}$ cm., would be

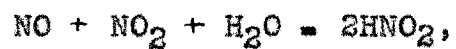
$$l = (\sqrt{2} \pi \sigma_{H_2O}^2 n_{H_2O})^{-1} = 6.3 \times 10^{-4} \text{ cm.}$$

and the ratio $Z_3/Z_2 = 5 \times 10^{-5}$. Multiplying by the value calculated for Z_2 gives $Z_3 = 8 \times 10^{19}$. Thus assuming that N_2O_3 is the participating species, approximately one ternary collision in twenty-five results in reaction.

While this is a comfortable margin from the standpoint of collision frequency, it must be observed that the requirement of a certain spatial configuration for the reaction complex might easily reduce the probability of reaction for each suitable collision by an order of magnitude. If this picture is to apply it is necessary to conclude that the energy of activation must be practically nil. This, of course, is a common characteristic of third order gas reactions and, in view of the probability that the heat of reaction (as well as the free energy change) is very small for this system, it is perhaps reasonable to expect it to hold here also.

Since the rate of the reverse reaction is of the same order of magnitude as that of the forward reaction and since the amounts of products and of reactants in equilibrium mixtures are comparable, the considerations given above apply equally well to the reverse process. A curious consequence of the third-order law is that water vapor is apparently a catalyst in the formation of an acid anhydride (N_2O_3) from the acid vapor.

It should perhaps be remarked that although the third-order hypothesis is reasonably satisfactory in explaining both kinetics and mechanism of the reaction



yet because of the rather limited range of the concentrations used in this study it cannot be regarded as well-established. The true explanation of the observed behavior may well be essentially more complex.

1. Johnston, H.S., Thesis, 1948, California Institute of Technology.
2. Melvin and Wulf, J. Chem. Phys. 3, 755 (1935).
3. Goodeve, Eastman and Dooley, Trans. Farad. Soc., 30, 1127 (1934).
4. Johnston and Giauque, J. Am. Chem. Soc. 51, 3194 (1929).
5. R.W. Engstrom, J. Optical Soc. Am., 37, 420 (1947).
6. E.F. Coleman, Electronics 19, 220 (1946).
7. E. Abel & E. Neusser, Monatshefte f. ch. 54, 855 (1929).
8. Verhoek & Daniels. J. Am. Chem. Soc., 53, 1250 (1931).
9. Forsythe and Giauque, J. Am. Chem. Soc., 64, 48 (1942).
10. W.N. Latimer, Oxidation Potentials, Prentice-Hall, (1938).
11. Lewis and Randall, Thermodynamics and the Free Energy of Chemical Substances, McGraw Hill, (1923).
12. Giauque & Kemp, J. Chem. Phys. 6, 40 (1938).
13. Hinshelwood, The Kinetics of Chemical Change, Oxford, 1940.

Propositions submitted by Lowell G. Wayne

Ph.D. Oral Examination, September 16, 1948, 1:00 P. M., Crellin Conference Room.
Committee: Professor Yost (Chairman), Professor Bates, Davidson, de Prima,
Kirkwood, Niemann.

1. a. A theorem which is illuminating in connection with the behavior of dissociating gases such as N_2O_4 may be stated as follows: in any system consisting of a gas and its gaseous dissociation products in equilibrium, where the heat of dissociation is sufficiently high, isentropic adiabatic expansion decreases the degree of dissociation.

b. As a corollary to this theorem it may be observed that for any such system there must exist a minimum temperature, below which exceptions to the behavior stated may not occur. This temperature is of the order of magnitude of $\Delta H/R$.

2. The objections of Krichevsky and Rosen to the Mayer statistical mechanical theory of critical point phenomena are not damaging to this theory. This paper illustrates a common failing in ascribing to nature continuity properties which though commonly observed, need not be universal.

Krichevsky and Rosen, *Acta Physicochimica USSR* 22, 153 (1947)

3. More elegant and more flexible than the usual derivation given for bond angles in s-p hybridization is a derivation utilizing direction cosines as co-ordinates for the angular parts of the wave functions and based on the recognition of the orthogonal character of the matrix involved in forming suitable sets of hybrid orbitals.

Pauling, "Nature of the Chemical Bond", p. 85; Ithaca, 1939.

4. The rate of dissociation of nitrogen tetroxide has been estimated by means of measurements of the velocity of sound and by the measurement of temperatures in a steady flow system. Results obtained by the former method are probably more reliable but they furnish only rather widely separated limits for the rate constant sought. I propose the application of the impact tube method (recently employed for the evaluation of relaxation times of various gases) for the more exact determination of this quantity.

Richards and Reid, *J. Chem. Phys.* 2, 193, 206 (1934)

Brass and Tolman, *J. Am. Chem. Soc.* 54, 1003 (1932)

Kantrowitz, *J. Chem. Phys.* 14, 150 (1946)

Huber and Kantrowitz, *J. Chem. Phys.* 15, 275 (1947)

5. A theory currently favored by meteorologists to account for the presence of cloud-forming nuclei in the atmosphere is that such nuclei consist of nitrous acid formed from the elements in the electrical discharge. I propose the consideration of nitric acid and nitrogen dioxide as each more likely to constitute such nuclei, on the basis of equilibrium considerations as well as comparison of chemical and physical characteristics of these substances. Experimental evidence is cited.

G. C. Simpson, *Quarterly J. Royal Meteorological Soc.* 67, 99 (1941)
Crane and Halpern, *Phys. Rev.* 56, 232 (1939)

6. Due to the neglect of the equilibrium $N_2O_3 + H_2O \rightleftharpoons 2HNO_2$, the values given by Abel and Neusser for $P_{HNO_2}/(HNO_2)$, the vaporization equilibrium constant, are too high by about 10% on the average. If corrected for this effect, their results permit the calculation of a value for the standard free energy of formation of nitrous acid (g) which would be sufficiently reliable to justify its inclusion in comprehensive tabulations such as those of Bichowski and Rossini.

Abel and Neusser, Monatshefte 54, 855 (1929)

Bichowski and Rossini, The Thermochemistry of Chemical Substances, Reinhold, New York, (1936)

7. The photochemical decomposition of N_2O_5 , sensitized by NO_2 , has not been observed for wave lengths of 4360 Å or more, even though NO_2 absorbs strongly at longer wave lengths. On the basis of the mechanism proposed by Ogg for the decomposition of nitrogen pentoxide it is to be predicted that the absorption of quanta by NO_2 in the system should accelerate the decomposition, even without preliminary photodissociation of the dioxide. I therefore propose a specific search for this effect, as bearing importantly on the correctness of the Ogg mechanism.

Baxter and Dickinson, J. Am. Chem. Soc., 51, 109 (1929)

R. A. Ogg, Jr., J. Chem. Phys. 15, 337 (1947)

8.a. Despite the fact that the reactions $2NO + Cl_2 = 2NOCl$, $2NO + Br_2 = 2NOBr$ and $Br_2 + Cl_2 = 2BrCl$ are all slow at room temperature, a mixture of the three gases nitric oxide, chlorine and bromine has been reported to reach equilibrium very rapidly. I propose a simple mechanism to account for this peculiarity, based on the postulated intermediate $NOCl_2$, which has previously been suggested to account for the third order kinetics of the reaction between NO and Cl_2 .

Yost and Russell, Systematic Inorganic Chemistry, p. 43 Prentice Hall, New York, 1944

Hinshelwood, Kinetics of Chemical Change, Oxford, London 1940

b. The multiplier phototube and oscilloscope should prove useful in investigating this hypothesis.

9. Smith reports that the gas phase reaction of nitric acid vapor with nitric oxide, $2HNO_3 + NO = 3NO_2 + H_2O$, is autocatalytic, following approximately the law $d(NO_2)/dt = (NO)(HNO_3)(NO_2)$, and that it is also catalyzed by water vapor without elimination of the time-lag (induction period). I propose a mechanism involving the intermediates N_2O_3 and HNO_2 to account qualitatively for the observed behavior.

J. H. Smith, J. Am. Chem. Soc. 69, 1741 (1947)

10. In view of the importance of water vapor as a chemical reagent from both the theoretical and the practical standpoint it is surprising that so little quantitative work has been done on the kinetics of reactions involving it. I propose that reactions such as the following should be studied, in the hope of obtaining a clearer insight into the mode of action of water vapor in homogeneous reactions.

(1) $I_2 + Cl_2 = IC_1$. Hildebrand has reported that in carbon tetrachloride solution this reaction is strongly catalyzed by water and that the "wet" reaction has a large negative temperature coefficient.

(2) $N_2O_5 + H_2O = 2HNO_3$. Smith and Daniels found that the rapid reaction between N_2O_5 and NO was strongly catalyzed by water vapor; since HNO_3 reacts with NO more rapidly than does N_2O_5 , the hydration reaction seems to be a probable first step in that process.

(3) $SO + H_2O = ?$ It is claimed that active sulfur monoxide is consumed by water vapor ten times as fast at 0° as at $40^\circ C$.

J. H. Hildebrand, J. Am. Chem. Soc. 68, 915 (1946)

Smith and Daniels, J. Am. Chem. Soc. 69, 1735 (1947)

N. M. Emmanuel, J. Phys. Chem. (U.S.S.R.) 19, 15 (1945)

(Chemical Abstracts 39, 3720)

11. Use of the letter system in grading undergraduates at California Institute of Technology may in some cases have an adverse effect on their future placement. I propose its abolition.